

A compact neutron spectrometer for neutrons produced by cosmic rays

E Jarvie¹, A Buffler¹, T Hutton¹, Z Ndabeni^{1,3}, R Nndanganeni² and C Vandevoorde³

¹ Department of Physics University of Cape Town, ² South African National Space Agency, ³ iThemba LABS

E-mail: JRVERI002@myuct.ac.za

Abstract. A compact neutron spectrometer consisting of a 6x6x50 mm³ plastic scintillator with pulse shape discrimination (PSD), a silicon photomultiplier and digital data acquisition has been developed. Results from the first characterisation measurements with this device using neutrons up to 14.1 MeV are discussed. The spectrometer showed good quality pulse shape discrimination and energy resolution. Work to optimise the detector and characterise it up to 100 MeV is currently ongoing.

1. Introduction

Cosmic radiation interacting with our atmosphere produces a host of secondary particles through spallation [1][2]. At aviation altitudes the radiation field is made up predominantly of fast neutrons in the energy range 1-100 MeV [3], as seen in figure 1. The neutron energy spectrum and dose rate at these altitudes is well studied in regular conditions, and several computational models exist to calculate these values [4]. However, these codes are relatively unverified in the Southern Hemisphere, and very little observational data exists during space weather events such as solar flares and coronal mass ejections since they are fairly rare and unpredictable. These events cause an increase in ionizing radiation which not only provides increased biological risk to air crew and passengers [5], but also increases the risk of soft errors in aircraft electronics [6]. In order to better understand the effect of space weather events on our atmosphere and risks associated with flying during such events, more observational data need to be acquired.

Currently, Tissue Equivalent Proportional Counters (TEPCs) are the standard instrument for air crew dose measurements [8], however these devices do not provide spectroscopic information and therefore do not provide neutron-specific dose. As the radiation field at aviation altitudes is comprised 40% of neutrons [2] this is a problem. Neutron spectroscopy in a mixed radiation field requires a device capable of discriminating between neutron and gamma ray events. In some organic scintillators this can be done using a technique known as pulse shape discrimination (PSD). Typically, spectroscopic measurements of neutrons are made with organic liquid scintillators due to their high quality PSD capabilities, however these detectors and their associated electronics are bulky, and are toxic and fire hazards. We discuss the characterisation of the first prototype of a compact neutron spectrometer intended for studying the neutron field in an aviation scenario. The device consisting of a plastic scintillator capable of PSD, silicon

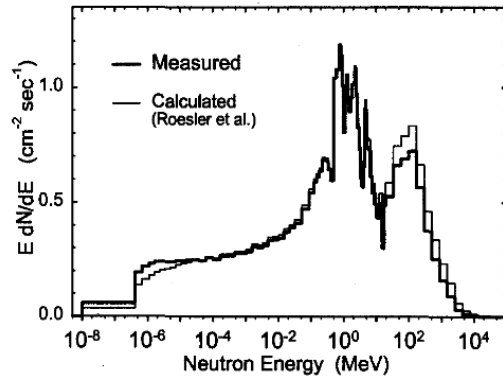


Figure 1. Neutron energy spectrum at an altitude of 20 km at 54°N, 117°W. The darker line is the measured spectrum by Goldhagen et al. [3] and the lighter line is the calculated spectrum at the same location produced by Roesler et al. [7].

photomultipliers and digital data acquisition, has been designed to be compact, robust and safe to operate on board aircraft.

2. Experimental setup

The prototype device consisted of a 6x6x50 mm³ slab of EJ276 plastic scintillator [9] coupled to a SensL C-series silicon photomultiplier (SiPM) [10] in a light tight polylactic acid plastic (PLA) casing, seen in figure 2, operated with an external power supply of 28.5 V. The signals produced by the detector were acquired digitally using a CAEN DT5730 digitiser [11] and custom open source software developed at UCT [12]. The EJ276 plastic scintillator was chosen since it is capable of PSD, is well characterised [13] and can be produced in any shape or size. The scintillator was wrapped in a reflective material in order to improve light collection from the scintillator. Since the intention is for this device to be operated on board commercial aircraft all features of the spectrometer were also chosen to make it safe to operate on board aircraft and pass through airport security checks without issues. The gamma ray and neutron response of the detector was characterised up to 4.3 MeV and 14.1 MeV respectively at the n-lab in the Department of Physics at UCT. Gamma ray characterisation was performed using ¹³⁷Cs, ²²Na and ⁶⁰Co sources and the neutron characterisation was performed using a 2.2 GBq americium beryllium (AmBe) source and 14.1 MeV neutrons from a D-T sealed tube neutron generator (STNG).

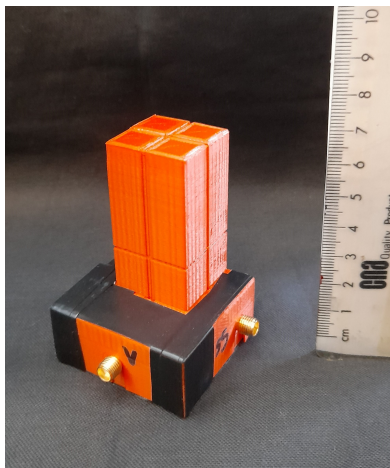


Figure 2. The prototype neutron detector scaled with a ruler measuring in centimetres.

3. Results and Analysis

Results from the prototype detector are compared to those of a reference detector (EJ301 liquid scintillator) which is commonly used for neutron spectroscopy. The fluorescence given off by scintillators is made up of a fast decaying and a slow decaying component. The ratio of light given off in each component, and therefore the shape of the pulse, depends on the nature of the excited particle [14]. Pulse shape discrimination uses this property to distinguish between gamma ray and neutron events since they interact through different mechanisms.

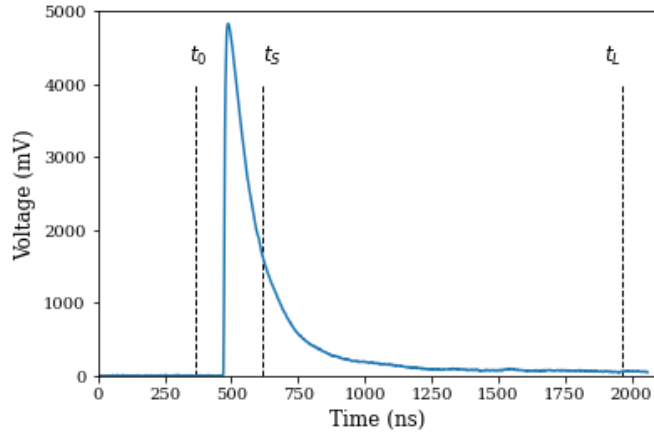


Figure 3. Typical pulse output from the prototype detector showing the starting time t_0 , short time interval t_S and long time interval t_L .

In this work the charge comparison method of PSD was implemented. The starting time, t_0 , for each pulse was chosen such that it was 80 ns before the peak of the pulse. It should be noted that using methods such as constant fraction discrimination (CFD) [12] or e-folding would be better approaches and will be implemented further in future work. The pulse was then integrated over a short time interval $[t_0; t_S]$ to produce Q_S – the short integral, and a long time interval $[t_0; t_L]$ to obtain Q_L – the long integral. The time t_L was chosen to occur at $t_0 + 1600$ ns so that the entire pulse is included and t_S was chosen to be $t_0 + 250$ ns such that the quality of the separation of pulses was optimised. As with the definition of t_0 , the definition of t_L would benefit from being determined using methods such as CFD. The chosen time intervals in relation to a typical pulse are shown in figure 3.

In the charge comparison method the pulse shape parameter S is determined through the following relation:

$$S = k \frac{Q_S}{Q_L} + c \quad (1)$$

where k and c are constants used to appropriately scale S . The gamma ray sources (^{22}Na , ^{137}Cs , ^{60}Co) were used for scaling Q_L to light output L , which has the units of MeV_{ee} (electron equivalent). Figures 4 and 5 show number of counts as a function of S and L for the AmBe source and STNG respectively. The loci associated with recoiling electrons from Compton scattering events of gamma-rays (e) and protons recoiling from n-p elastic scattering of neutrons (p) are well separated over the full range of L .

The separation between the distributions of S for two pulse classes events is quantified by the figure of merit (FoM). If the proton (p) and electron (e) recoil distributions are Gaussian the FoM can be defined in terms of the mean (μ) and full width half maximum (FWHM) such that

$$\text{FoM} = \frac{|\mu_e - \mu_p|}{\text{FWHM}_e + \text{FWHM}_p}. \quad (2)$$

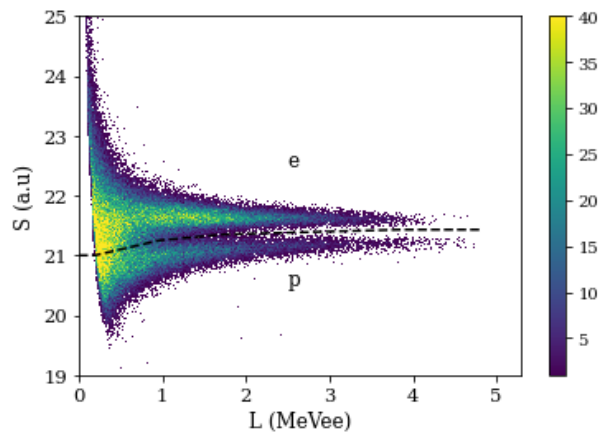


Figure 4. Counts as a function of L and S for events in the prototype detector when exposed to the AmBe source. The loci associated with neutron (e) and gamma ray (p) events are indicated and the events were separated along the dashed line.

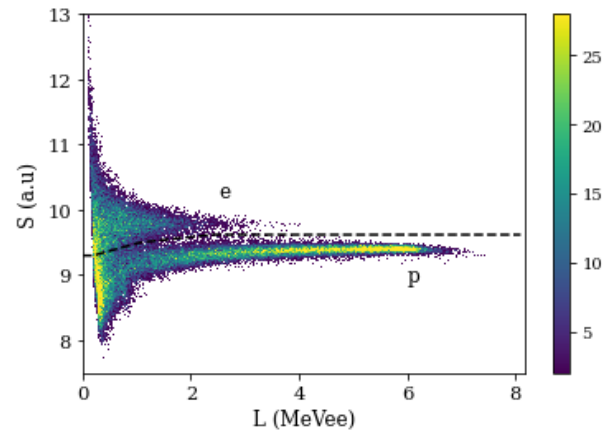


Figure 5. Counts as a function of L and S for events in the prototype detector when exposed to the STNG. The loci associated with neutron (e) and gamma ray (p) events are indicated and the events were separated along the dashed line.

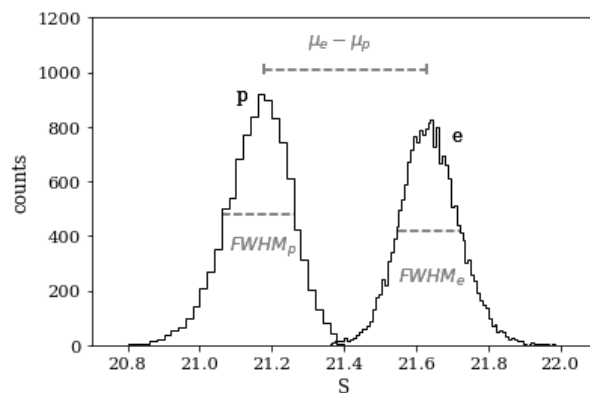


Figure 6. Counts as a function of pulse shape S for $1.9 < L < 5.0$ MeV_{ee} from the measurements of the AmBe source with the prototype detector. The gamma ray (e) and neutron (p) events are indicated.

The prototype detector has a FoM of 1.2 ± 0.4 over the light output range $1.9 < L < 7.7$ MeV_{ee}, this is lower than that of the reference detector which has a FoM of 2.5 ± 0.2 over the same light output range. Despite the comparatively lower quality, a FoM > 1 is considered acceptable for the intended purpose of the detector.

To obtain spectroscopic information from the data the neutron light output spectra (LOS) were unfolded using the MAXED and GRAVEL algorithms [15]. The unfolding process utilises minimization algorithms which find the optimum combination of response functions required to produce the measured LOS provided. From this the algorithm can infer the energy spectrum of the radiation field. In order to unfold the measured LOS for the prototype detector the spectrum had to be scaled to match the response function of the EJ301 detector since there no response functions exist for the prototype.

Figures 7 and 8 show the comparison of the AmBe light output and energy spectra for the prototype and reference detectors. In figure 8 the energy spectra have peaks at the same energies, however show some differences in fluence which results in the spectra having slightly different shapes, particularly towards lower energies. This is seen in the LOS in figure 7 at low L where there is there is a separation between the two spectra.

Similarly, figures 9 and 10 show the light output and energy spectra for measurements of the 14.1 MeV neutrons from the STNG. In figure 10 the 14.1 MeV energy spectra clearly agree well on the position of the energy peak, however there are two distinct discrepancies in the spectra. At high energies ($\sim 15 - 16.5$ MeV) the spectrum produced by prototype has some extra contributions which is due to event pile-up in the prototype. This feature is seen in the LOS in figure 9 as a slightly longer tail at roughly 8.2 MeV_{ee}. The small bump at 11 MeV_{ee} in the energy spectrum from the prototype detector is due to the response function used having a slightly different shape to the measured LOS. The difference in shape, which is seen at around 6.5 MeV_{ee} in the LOS, is because the response function used is for a larger detector in which multiple scatter occurs. Since the prototype is very small there are no double scatter events.

Overall, the energy spectra of the two detectors agree well in terms of key features such as position of energy peaks. All of the differences in the unfolded energy spectra can be corrected by producing a response matrix for the prototype detector and using it for the unfolding.

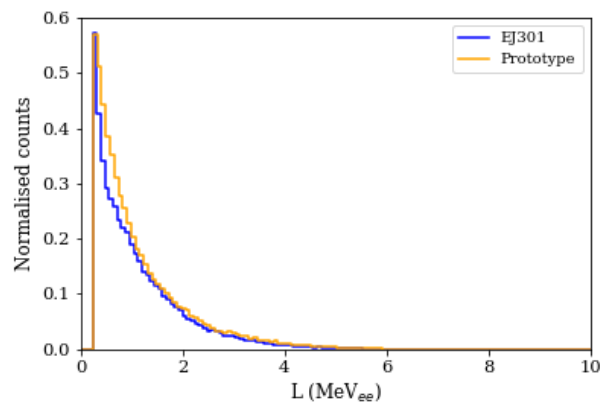


Figure 7. AmBe neutron light output spectrum for EJ301 reference detector and prototype detector.

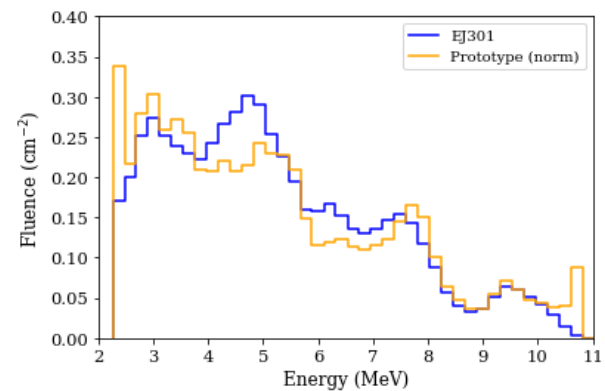


Figure 8. Unfolded AmBe neutron energy spectrum for the EJ301 reference detector and prototype detector.

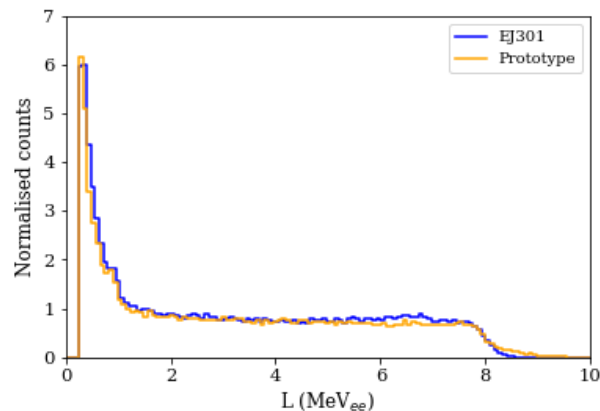


Figure 9. STNG (14.1 MeV) neutron light output spectrum for EJ301 reference detector and prototype detector.

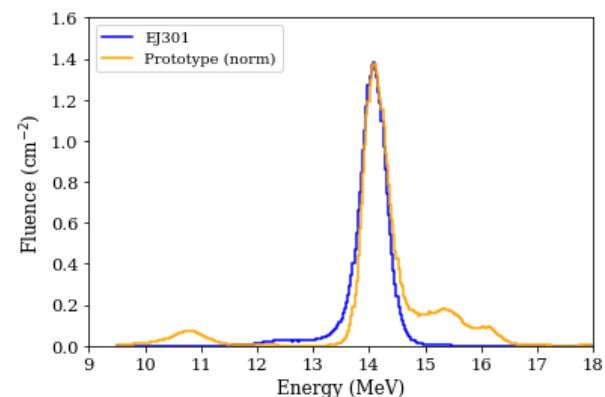


Figure 10. Unfolded STNG neutron (14.1 MeV) energy spectrum for the EJ301 reference detector and prototype detector.

The relative efficiency of the prototype detector was determined by comparing the detected

neutron rate to that measured in the EJ301 detector for the same source conditions. From Table 1 it is clear that the prototype has a lower efficiency comparison to the reference detector, however this is expected for a detector of this size since the scintillator is smaller. The energy peak resolution for the 14.1 MeV neutrons is comparable for the two detectors, which implies that the prototype is capable of high quality spectroscopy. In the work done previously by Comrie [12] a detector consisting of a EJ299-33 plastic scintillator of the same dimensions coupled to two SiPMs was presented. In comparison to this detector system the prototype does not perform as well, with a lower efficiency and FoM, however it is suggested in Comrie's work that the addition of the second SiPM improved both of these characteristics significantly.

Table 1. Comparison of the EJ301 reference and prototype detectors for relative neutron efficiency of both sources and 14.1 MeV energy peak resolution.

	EJ301	Prototype
Relative neutron efficiency (AmBe)	1.00	0.38
Relative neutron efficiency (STNG)	1.00	0.15
14.1 MeV energy peak resolution	1.64 ± 0.09	1.63 ± 0.08

4. Conclusions and future work

Overall the compact spectrometer shows promise. However improvements to the design and characterisation at higher energies are needed. Work is currently underway to improve and optimise the design of the detector presented using GEANT4 simulations. In addition to this, the next detector design will likely feature two SiPMs in order to improve light collection which will improve detection efficiency and PSD quality. The updated detector will be characterised with neutrons over the full energy range of interest at the UCT n-lab (1-14 MeV), AMANDE fast neutron facility at the IRSN in France (1-20 MeV) and iThemba LABS fast neutron facility (30-100 MeV). Measurements will also be made in real in-flight scenarios on both local and international flights.

Acknowledgments

This work is supported by the National Research Foundation (South Africa) and the South African National Space Agency.

References

- [1] Grieder P 2001 *Cosmic Rays at Earth: Researcher's reference manual and data book* (Elsevier)
- [2] Buffler A 2019 Neutrons in space Tech. rep. Seminar at South African National Space Agency
- [3] Goldhagen P, Clem J and Wilson J 2004 *Rad. Prot. Dosim.* **110** 387
- [4] Clem et al 2004 *Rad. Prot. Dosim.* **110** 423–428
- [5] Lynge E 2001 *International journal of epidemiology* **30** 830–832
- [6] W Tobiska et al 2015 *Space weather* **13** 202–210
- [7] Roesler S, Heinrich W and Schraube H 2002 *Radiat. Prot. Dosim.* **98** 367–388
- [8] Bilski P, Olko P and Horwacik T 2004 *Nukleonika* **49** 77–83
- [9] Eljen technologies, products <https://eljentechnology.com/products/plastic-scintillators/ej-276>
- [10] Sensl c-series data sheet <https://sensl.com/downloads/ds/DS-MicroCseries.pdf>
- [11] Caen desktop digitizers <https://www.caen.it/desktop-digitizers/>
- [12] Comrie A 2016 *A new compact neutron spectrometer* Ph.D. thesis University of Cape Town
- [13] Buffler A, Comrie A, Smit F and Wortche H 2015 *IEEE Transactions on nuclear science* **62** 1422–1428
- [14] Knoll G 2010 *Radiation Detection and Measurement* (Wiley)
- [15] Reginatto M, Goldhagen P and Neumann S 2002 *Nucl. Instr and Meth. A* **476** 242–246